Conference materials
UDC 535.135
DOI: https://doi.org/10.18721/JPM.153.334

Optical second-harmonic response of an axially-symmetric medium under radially polarized excitation

S. A. Scherbak [1, 2]✉, I. V. Reshetov [1, 2], A. A. Lipovskii [1, 2]

[1] Alferov University, St. Petersburg, Russia;

[2] Peter the Great St. Petersburg Polytechnic University, St. Petersburg, Russia

✉ Sergeygtn@yandex.ru

Abstract. We simulated optical second harmonic response, both surface and bulk, of axially symmetric media excited by tightly focused radially polarized fundamental beams. The modeling showed a highly localized character of second harmonic generation. We estimated decrease of overall second harmonic signal for defocusing of fundamental beam relatively to a sample's surface. Radiation patterns of second harmonic waves were compared for different numerical apertures of a focusing objective, for different focus shift relatively to the sample's surface and for surface and bulk second harmonic responses. The model developed is applicable for second harmonic generation by interfaces, films and poled glasses.

Keywords: nonlinear optics, second harmonic generation, radial polarization, axisymmetric medium, modeling

Funding: This study was funded by within the framework of the Russian Science Foundation project No. 21-72-00048 "Non-synchronous nonlinear optical phenomena in micro- and nanostructures using light waves with non-trivial polarizations", research project No. 21-72-00048.

Citation: Scherbak S. A., Reshetov I. V., Lipovskii A. A., Optical second-harmonic response of an axially-symmetric medium under radially polarized excitation. St. Petersburg State Polytechnical University Journal. Physics and Mathematics, 15 (3.3) (2022) 177–181. DOI: https://doi.org/10.18721/JPM.153.334

Материалы конференции
УДК 535.135
DOI: https://doi.org/10.18721/JPM.153.334

Генерация второй оптической гармоники осесимметричной средой под воздействием радиально поляризованного излучения

С. А. Щербак [1, 2]✉, И. В. Решетов [1, 2], А. А. Липовский [1, 2]

[1] Санкт-Петербургский национальный исследовательский Академический университет имени Ж. И. Алферова Российской академии наук, Санкт-Петербург, Россия;

[2] Санкт-Петербургский Политехнический университет Петра Великого, Санкт-Петербург, Россия

✉ Sergeygtn@yandex.ru

Аннотация. Проведено моделирование генерации второй гармоники поверхностью и объемом осесимметричного образца, освещенного сильно сфокусированным радиально поляризованным световым лучом. Исследованы влияния числовой апертуры фокусирующего объектива, толщины нелинейного слоя и положения фокуса относительно поверхности образца на генерацию второй гармоники. В частности, проведено сравнение диаграмм направленности излучения в этих случаях, показан высоко локализованный характер генерации второй гармоники. Разработанная модель подходит для анализа генерации второй гармоники интерфейсами, тонкими нелинейными пленками и поляризованной областью стекла.

Ключевые слова: нелинейная оптика, генерация второй гармоники, радиальная поляризация, осесимметричная среда, моделирование

Финансирование: Работа выполнена в рамках проекта РНФ № 21-72-00048 «Несинхронные нелинейно-оптические явления в микро- и наноструктурах при использовании световых волн с нетривиальными поляризациями».

Ссылка при цитировании: Щербак С. А., Решетов И. В., Липовский А. А. Генерация второй оптической гармоники осесимметричной средой под воздействием радиально поляризованного излучения // Научно-технические ведомости СПбГПУ. Физико-математические науки. 2022. Т. 15. № 3.3. С. 177–181. DOI: https://doi.org/10.18721/JPM.153.334

Introduction

It is known that radially polarized light waves focused with a high numerical aperture (NA) objective acquire a significant longitudinal component of electric field near the focal plane [1]. This allows applications of vector light beams in nanoparticles' trapping and delivering [2, 3], dark-field imaging and visualization down to a single molecule [4, 5], laser material processing [6]. Also, this peculiar distribution of electric field can provide a nonlinear optical response that differs significantly from that typical for trivially polarized excitations. Particularly, this allows observation of second order nonlinearity of highly symmetrical (e.g., axial) structures under normal incidence. In nonlinear optics of vector light beams, studies of second harmonic generation (SHG) by a material with symmetry $\bar{4}3m$ [7], surface and bulk SHG, including spatially resolved experiments, by glasses [8, 9] and thin nonlinear films [10] were reported.

In this study, we developed a model that describes both surface and bulk second harmonic (SH) response of an axially symmetric medium under tightly focused radially polarized excitation. The model is applicable for SH generation by interfaces, films and poled glasses.

Theory

We consider a radially polarized light beam falling normally (along z-axis) to a focusing objective and then to the interface between two media with indices n_1 and n_2. Resulting equations (in cylindrical coordinates) for components of the second harmonic electric field in the far-field zone in the direction defined by the polar angle θ are:

$$E_{\rho}^{2\omega}(\theta) = P_1 \sin\theta\cos\theta - P_2 \sin^2\theta + P_2 \quad (1)$$

$$E_{z}^{2\omega}(\theta) = P_1 \cos^2\theta - P_2 \sin\theta\cos\theta - P_1 \quad (2)$$

where parameters P_1 and P_2 are:

$$P_1 = 2\pi \int_0^{+\infty} rdr \int_{z_0}^{z_1} dz P_{\perp}(r,z) J_0(Kr\sin\theta) e^{iKz\cos\theta} \quad (3)$$

$$P_2 = 2\pi i \int_0^{+\infty} rdr \int_{z_0}^{z_1} dz P_{\parallel}(r,z) J_1(Kr\sin\theta) e^{iKz\cos\theta} \quad (4)$$

z_0 is the sample interface coordinate, z_1 is the coordinate of the rare side of the nonlinear layer, K – wavenumber vector of the SH wave. Components of nonlinear polarizability **P** are connected with components of the fundamental electric field via nonlinear constitutive equations. For axially symmetric media, these are:

$$P_{\perp} = \chi_{\perp\perp\perp} E_z^2 + \chi_{\perp\parallel\parallel} E_r^2 \quad (5)$$

$$P_{\parallel} = \chi_{\parallel\perp\parallel} E_z E_r \quad (6)$$

where $\chi_{\perp\perp\perp}$, $\chi_{\parallel\perp\parallel}$ and $\chi_{\perp\parallel\parallel}$ are nonzero components of the second order susceptibility tensor χ. Surface nonlinearity can be considered using substitution $\chi \to \chi^{surf}\delta(z\text{-}z_0)$, where $\delta(z\text{-}z_0)$ is the Dirac δ-function. Expressions for the distribution of the fundamental electric field of a radially polarized light wave, E_z and E_r, near the focal plane are presented in Ref. [7].

Squared modulus of SH field, which components are described by Eqs. (1-2), gives intensity of the radiated SH signal:

$$I_{2\omega}(\theta_2) = \left|T_p^{n_2 \to n_1}(\theta_2)\right|^2 \left(\left|E_\rho^{2\omega}(\theta_2)\right|^2 + \left|E_z^{2\omega}(\theta_2)\right|^2\right) \quad (7)$$

In Eq. (7) we took into account that output SH radiation refracts at the rear side of the sample. Thus, we added the Fresnel's transmission coefficient $T_p^{n_2 \to n_1}$ and represented the intensity as a function of the refraction angle θ_2, which related to θ via the refraction law: $n_2 \sin\theta = n_1 \sin\theta_2$. Integration of Eq. (7) over θ_2 allows obtaining total SH intensity.

Results and Discussion

In calculations, we considered fundamental wavelength of 1064 nm, $n_1 = 1$, $n_2 = 1.51$, $z_0 = z_f = 0$, where z_f is the objective focus coordinate, and suppose $\chi_{\perp\perp\perp} = 3\chi_{\parallel\perp\parallel} = 3\chi_{\perp\parallel\parallel}$. This relation between the components of χ is a so-called "1/3 rule" which is common for poled glasses [11]. For surface nonlinearity we calculated SH radiation patterns for different NA's of focusing objective, see Fig. 1.

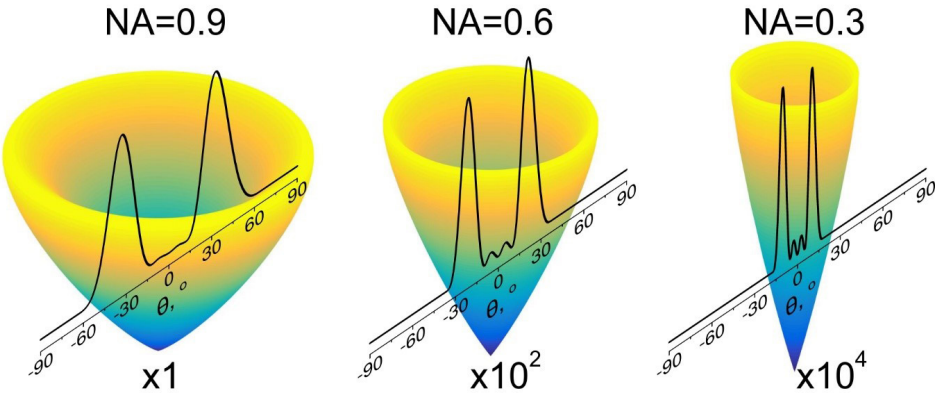

Fig. 1. SH radiation patterns for NA's of focusing objective: 0.9 (left), 0.6 (middle), 0.3 (right). Intensity scaling factor is denoted below each pattern. Overlaying curves – patterns cross-sections

In Fig. 1 we observe characteristic SH radiation patterns for the case of "1/3 rule". The patterns, expectedly axially symmetric, represent a single empty cone, which corresponds to a two-lobed pattern in a cross-section (see overlaying curves in Fig. 1). For tight focusing (NA = 0.9) the pattern is relatively broad with cone's full angle about 33°. For weaker focusing (NA = 0.6 and NA = 0.3) the pattern is noticeably narrower – for NA = 0.6 angle is ~ 23°, for NA = 0.3 – about 10°. Note, these angles decrease with the aperture angles of the objectives, which are about 65°, 37° and 17° , respectively, for NA = 0.9, 0.6 and 0.3. Also, inner (closer to normal) lobes, which are barely seen for NA = 0.9, becomes more evident, though still about an order lower in magnitude than the outer ones. The overall SH radiation intensity for NA = 0.3 is about four orders of magnitude less than for NA = 0.9.

For tight focusing (NA = 0.9) we calculated SH signal depending on focus shift z_f relatively to the nonlinear interface. The dependence presented in Fig. 2, *a* demonstrates a symmetric peak with a half-width of ~ 2 μm, i.e. 1-μm focus shift from the surface results in two-fold decrease of the overall SH signal. For 3-μm focus shift, the decrease is 10-fold. Note, for smaller NAs this dependence is broader and the SH signal – lower. This was expected for lower intensity in focus and longer caustic produced by weaker objectives. Also, we estimated evolution of radiation patterns with focus shift (see insets in Fig. 2). The radiation pattern for exact focusing ($z_f = 0$) is the same as one presented in Fig. 1. For higher focus shifts (e.g., $z_f = 4$ μm), the pattern broadens and obtains a noticeable inner shoulder. Because of this changes, for a material with a known

relation of components of χ, the shape of the SH radiation pattern can be another criterion of the focusing. Similar dependence for bulk subsurface nonlinear layer of thickness d_{NL} = 8 μm is presented in Fig. 2, *b* with radiation patterns as insets. The dependence of SH signal on focus shift in this case has a shape of an asymmetric peak, which is, expectedly, broader than in the case of surface nonlinearity. Also, focus position providing the maximal SH signal, $z_f \approx 1.4$ μm, is closer to the surface ($z_0 = 0$) than to the rear border of the nonlinear layer ($z_1 = 8$ μm). This is because of the refraction of the fundamental beam at the interface ($n_1 = 1/n_2 = 1.51$). Half-width of this dependence is ~ 4 μm. Thus, such dependencies can allow estimating thickness of nonlinear layers. In this case, the radiation pattern also changes with focus shift: for the optimal focusing ($z_f \approx 1.4$ μm) it is similar to one of surface nonlinearity, for a higher focus shift (e.g., $z_f = 6$ μm) the pattern broadens and obtains an outer shoulder (see the insets in Fig. 2, *b*).

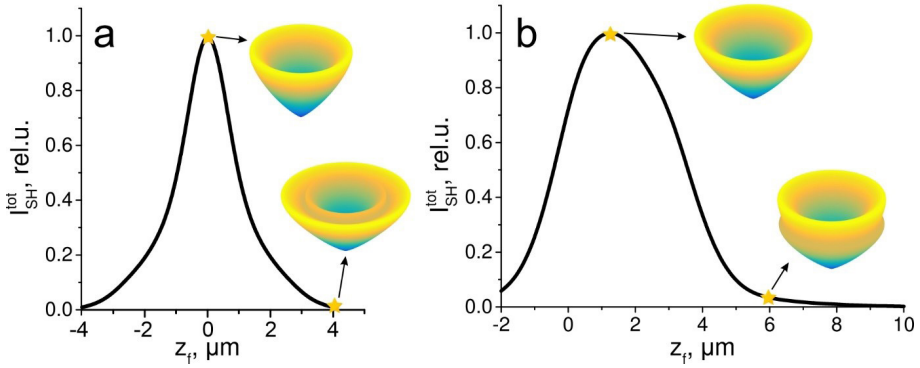

Fig. 2. Total signal of SH generation by surface nonlinearity (*a*) and subsurface nonlinear layer of thickness d_{NL} = 8 μm vs focus shift from the surface (*b*)

In Fig. 3, *a* we demonstrate total SH signal for nonlinear layer vs thickness of this layer, dNL, for the tight focusing case (NA = 0.9). The signal expectedly increases with the thickness and then saturates, since the excitation is localized. Note, for the non-localized regime of SHG under unfocused excitation, total SH signal depends on the thickness of nonlinear layer quadratically. Dependence of SH intensity vs. $(d_{NL})^2$ for NA = 0.3, which presented in Fig. 3, *b*, is close to a linear one that confirms the latter statement. The calculated dependence slightly bends relatively to an exact line (dashed one). This is probably because the objective with NA = 0.3 provides rather weakly focused beam than unfocused. In the insets in Fig. 3, *a* we schematically present radiation patterns of SH waves for different thickness of the nonlinear layer. The patterns are similar to one of surface nonlinearity, though, for thicker layers, they broaden. Cones angles are denoted in the insets. This broadening can allow distinguishing surface nonlinearity from bulk one.

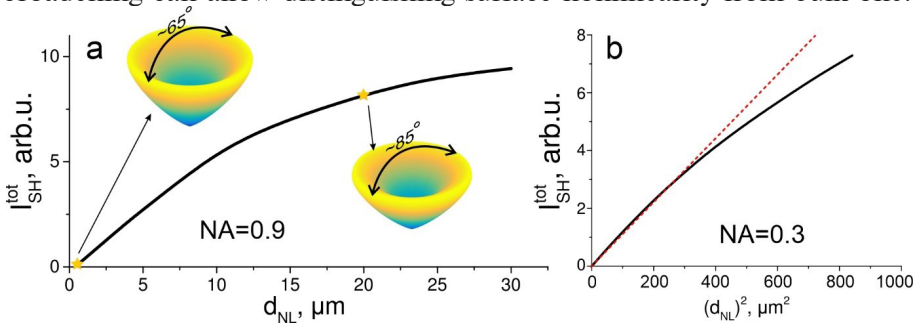

Fig. 3. Total signal of SH generation by differently thick subsurface nonlinear layers for NA = 0.9 (*a*) and NA=0.3 (*b*). Dotted line in (*b*) represents an exact quadratic dependence and no more than guide for eyes

Conclusion

We developed a model for surface and bulk optical second harmonic response of axially symmetric medium under tightly focused radially polarized excitation. For relation between components of second order susceptibility tensor, we calculated SH radiation patterns for different NA of the focusing objective. It is demonstrated that the patterns have a shape of an empty cone and for higher NA (tighter focusing) magnitude of overall SH signal increases and the pattern

significantly broadens. For tight focusing, we estimated decrease of SH signal when the focus position shifts from the surface – 3 μm shift corresponds to an order drop in the SH intensity. We showed that for tight focusing intensity of SH saturates with increase in the thickness of nonlinear layer, that corresponds to local excitation of SHG.

REFERENCES

1. **Hao B., Leger J.,** Experimental measurement of longitudinal component in the vicinity of focused radially polarized beam, Optics Express. 15 (2007) 3550.

2. **Zhan Q.,** Trapping metallic Rayleigh particles with radial polarization, Optics Express. 12 (2004) 3377.

3. **Kawauchi H., Yonezawa K., Kozawa Y., Sato S.,** Calculation of optical trapping forces on a dielectric sphere in the ray optics regime produced by a radially polarized laser beam, Optics Letters. 32 (2007) 1839.

4. **Biss D. P., Youngworth K. S., Brown T. G.,** Dark-field imaging with cylindrical-vector beams, Applied Optics. 45 (2006) 470.

5. **Novotny L., Beversluis M. R., Youngworth K. S., Brown T. G.,** Longitudinal Field Modes Probed by Single Molecules, Physical Review Letters. 86 (2001) 5251–5254.

6. **Drevinskas R., Zhang J., Beresna M., Gecevičius M., Kazanskii A. G., Svirko Y. P., Kazansky P. G.,** Laser material processing with tightly focused cylindrical vector beams, Applied Physics Letters. 108 (2016) 221107.

7. **Ohtsu A.,** Second-harmonic wave induced by vortex beams with radial and azimuthal polarizations, Optics Communications. 283 (2010) 3831–3837.

8. **Wang X., Fardad S., Das S., Salandrino A., Hui R.,** Direct observation of bulk second-harmonic generation inside a glass slide with tightly focused optical fields, Physical Review B. 93 (2016) 1–5.

9. **Wang X., Shen S., Sun J., Fan F.,** Chang S., Surface and bulk second-harmonic responses from a glass slide using tightly focused radially polarized light, Optics Letters. 41 (2016) 5652.

10. **Biss D. P., Brown T. G.,** Polarization-vortex-driven second-harmonic generation, Optics Letters. 28 (2003) 923.

11. **Kazansky P. G., Russel P. S. J.,** Thermally poled glass: frozen-in electric field or oriented dipoles?, Optics Communications. 110 (1994) 611–614.

THE AUTHORS

SCHERBAK Sergey A.
sergeygtn@yandex.ru
ORCID: 0000-0002-0507-5621

LIPOVSKII Andrey A.
lipovskii@mail.ru
ORCID: 0000-0001-9472-9190

RESHETOV Ilya V.
reshetov_iv@spbstu.ru
ORCID: 0000-0002-8661-3654

Received 22.07.2022. Approved after reviewing 27.07.2022. Accepted 30.07.2022.